C.P. No. 1130

MINISTRY OF TECHNOLOGY

AERONAUTICAL RESEARCH COUNCIL

CURRENT PAPERS

Experimental Investigation of the Effect of Trailing-Edge Sweepback on the Subsonic Longitudinal Characteristics of Slender Wings

by

D. L. I. Kirkpatrick and A. G. Hepworth

Aerodynamics Dept., R.A.E., Farnborough

LONDON: HER MAJESTY'S STATIONERY OFFICE

1970

PRICE 8s 6d [42½p] NET

R 40499

R 40499

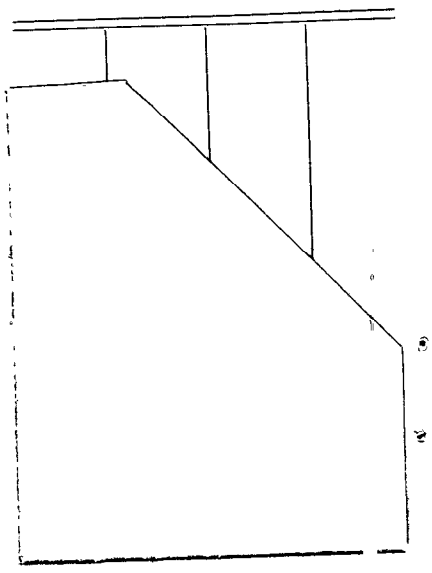

U.D.C. 533.693.3 : 533.6.013.412 : 533.691.2 : 533.6.013.12 :
533.6.013.13 : 533.6.013.152 : 533.6.011.32

C.P. No. 1130*
March 1970

EXPERIMENTAL INVESTIGATION OF THE EFFECT OF TRAILING-EDGE SWEEPBACK ON THE SUBSONIC LONGITUDINAL CHARACTERISTICS OF SLENDER WINGS

by

D. L. I. Kirkpatrick

A. G. Hepworth

Aerodynamics Dept., R.A.E., Farnborough

SUMMARY

This Report presents the results of an experiment to measure the lift, drag and pitching moment characteristics of three slender ogee wings with different trailing-edge sweepback angles. Analysis of these results shows how the characteristics of wings with swept trailing edges can be correlated with those of wings with unswept trailing edges.

*Replaces R.A.E. Technical Report 70039 - A.R.C. 32237.

CONTENTS

1 INTRODUCTION

The supersonic cruise characteristics of slender wings may be predicted theoretically, but the characteristics at the subsonic speeds and high incidences associated with take-off and landing cannot be predicted with acceptable accuracy by the existing theories, none of which take account of both the effects of the development of leading-edge vortices and the need to satisfy the Kutta condition at the trailing edge. Consequently several experimental investigations[1,2] have been made to obtain sufficient data to identify the effects of various planform parameters on the performance and stability of slender wings and the most rigorous and comprehensive of these investigations has shown[2] how the subsonic longitudinal characteristics of a series of slender wings with various planform shapes and slenderness ratios can be correlated.

Peckham[1] investigated the effect on the longitudinal characteristics of a flat plate with a gothic planform of varying the sweepback of the trailing edge from -15 to 56.3 deg, but in his experiment the effects of sweepback might have been distorted by the variation with sweepback of wing camber produced by the asymmetrical chamfer at the edges of the flat-plate wings tested. Kirby[2] measured the effect on the lift and pitching moment on an uncambered ogee wing of changing the trailing-edge sweepback from 0 to 14.4 deg, but pointed out that more tests would be required before the effect of trailing-edge sweepback could properly be assessed.

The experiment presented in this Report was made to investigate the effect on the longitudinal characteristics of an uncambered ogee wing of varying the trailing-edge sweepback angle from 5 to -15 deg (see Fig.1). This Report describes the experimental procedure and the analysis of the results to discover whether the characteristics of slender wings with swept trailing edges could be correlated, using Kirby's method[2], with those of wings with straight trailing edges.

2 DETAILS OF MODELS AND TESTS

Each of the three uncambered wings tested had an ogee planform and the shape of its leading edge was defined by the equation

$$\frac{y}{b/2} = 0.746\left(\frac{x}{c_o}\right) + 0.841\left(\frac{x}{c_o}\right)^4 - 0.587\left(\frac{x}{c_o}\right)^7 \quad ,$$

where c_o was the centre-line chord for zero trailing-edge sweepback, x was the chordwise distance from the apex and y was the spanwise distance from the centre line to the leading edge. The wings had trailing-edge sweepback angles of 5, -5 and -15 deg, as shown in Fig.1. The shape of each chordwise cross-section of each of the three wings was the same and was specified in terms of the chordwise distance x' from the leading edge and the local chord c by the equation

$$\frac{z}{c} = \pm 0.05934 \frac{x'}{c}\left(1 - \frac{x'}{c}\right)\left[1 - 0.1\frac{x'}{c} + 1.2\left(1 - \frac{x'}{c}\right)^5\right] ,$$

where z was the distance from the chordal plane to the wing surface. The maximum thickness/chord ratio for each wing was therefore 0.030. The main geometric parameters describing the three wings are tabulated in Table 1.

The wings were mounted successively on a conventional wire rig in the 4ft × 3ft low-turbulence wind-tunnel at the R.A.E., Farnborough. The lift, drag and pitching moment on each wing were measured on the overhead balance at one degree intervals over an incidence range from +5 to +25 deg and, to define the characteristics at low incidence, at half degree intervals from -5 to +5 deg. All the tests were made at a free stream velocity of 71 m/sec (199.25 ft/sec), referred to for convenience as 200 ft/sec throughout this Report, and a Reynolds number of 2.1 million based on c_o.

The lift, drag and pitching moment coefficients were calculated from the experimental results by dividing the measured forces and moments by $q\,S$ and $q\,S\,c_c$ respectively, where q is the freestream dynamic pressure, S is the plan area bounded by the wing leading and trailing edges and c_c is the wing centre-line chord. The coefficients were then corrected for the effects of wind-tunnel blockage[3] and constraint[4] and the fully-corrected results are tabulated in Tables 2 to 4.

3 ANALYSIS OF RESULTS

3.1 Lift

The calculated values of the lift coefficient were plotted against incidence in Fig.2, which shows that at any angle of incidence the value of C_L decreases as the trailing-edge sweepback angle decreases; this variation is in accordance with the results obtained earlier by Peckham[1] and Kirby[2]. The insert in Fig.2 shows that at a typical incidence of 15 deg the value of

$L/q = S C_L$ increases as the trailing-edge sweepback decreases and more surface area is added at the rear of the wing, but the percentage increase in L/q is much less than the percentage increase in wing area.

3.2 Normal force

The aerodynamic characteristics of these three wings with swept trailing edges were analysed to discover whether their characteristics could successfully be correlated, using Kirby's method[2], with those of wings with straight trailing edges. For this analysis the normal force coefficient was calculated from the measured lift and drag coefficients using the expression

$$C_N = C_L \cos \alpha + C_D \sin \alpha \quad .$$

The normal force coefficient of a slender wing may be written

$$C_N = C_{N_{linear}} + C_{N_{non\text{-}linear}} = a\,\alpha + C_{N_{non\text{-}linear}} \quad ,$$

where a is the slope of the normal force characteristic at zero incidence. To find the value of this slope for each wing, the calculated values of C_N/α for that wing were plotted against incidence (see Fig.3) and a smooth curve was drawn through the plotted points to intercept the C_N/α axis at the value a. Because C_N and α tend to zero together the low-incidence end of the C_N/α characteristics could not be precisely defined but, by using values of C_N/α measured at both positive and negative incidences, it was possible to obtain values of a which are unlikely to be in error by more than ±2%. Kirby has shown[2] that the values of a for a series of slender wings with various planforms and straight trailing edges all lie on a single curve when plotted against a modified aspect ratio parameter $A\,(1 + c_{0.99}/c_c)$, where c_c is the centre line chord of the wing and $c_{0.99}$ is the local chord at 99% of the semispan. The values of a obtained from Fig.3 were plotted against this parameter in Fig.4 which shows that the value of a for a slender wing is not significantly affected by the sweepback angle of its trailing edge over the range of sweepback angle tested, and that the interpolated value for $\phi = 0$ is very close to the curve[2] correlating the results of wings with straight trailing edges. Consequently the linear component of the normal force coefficient on a slender wing with swept trailing edges can be estimated accurately by assuming that $a(\phi) = a(0)$, the

value of a obtained from the correlating curve[2] for a wing with the same leading-edge planform and a straight trailing edge.

Fig.5a shows that, as the trailing-edge sweepback angle changes from 5 to -15 deg, the non-linear component $C_{N_{NL}} = \alpha \left(\frac{C_N}{\alpha} - a \right)$ of the normal force coefficient decreases. Examination of this decrease of $C_{N_{NL}}$ and the concurrent increase in the wing area S showed that $q S C_{N_{NL}}$ the non-linear component of the normal force remained virtually constant as the trailing-edge sweepback altered. Fig.5b presents the results in the form used in Ref.2 and shows that $C_{N_{NL}}$ for each of the three wings tested is slightly larger than the values calculated using Kirby's method[2] for an ogee wing with the same leading-edge shape and an unswept trailing edge. This slight difference probably occurs because the thickness $\left(\frac{t}{c} = 0.030 \right)$ of the three wings tested was less than the thickness $\left(\frac{t}{c} = 0.04 \right)$ of Kirby's series of wings[2]; a similar increase of the non-linear component with decreasing thickness was discussed in Ref.2.

3.3 Drag

Although these tests were primarily concerned with the effect of trailing-edge sweepback on the position of the aerodynamic centre and therefore the drag was not measured with the techniques and accuracy necessary for a rigorous drag analysis, the calculated values of the lift-dependent drag factor have been presented to show the principal effect of trailing-edge sweepback on drag. The calculated values of the drag coefficient C_D were plotted in Fig.6 which shows that at large values of C_L the drag of the wing with positive trailing-edge sweepback is slightly less than the drag on the other two wings. The lift-dependent drag factor $K = \pi A (C_D - C_{D_o})/C_L^2$ was then calculated, by ignoring the drag values measured at low incidences, at which boundary-layer transition occurred near the trailing edge, and using values of C_{D_o} obtained by extrapolation of the drag values measured at moderate incidences, at which the boundary layer over most of the wing was turbulent, and was plotted against the lift coefficient in Fig.7. Fig.7 shows that, as the trailing-edge sweepback angle decreases and the aspect ratio decreases accordingly, the value of K decreases but the value of $K/A = \pi (C_D - C_{D_o})/C_L^2$ increases.

3.4 Pitching moment

The calculated values of the pitching moment coefficient about a point in the chordal plane and 0.617 c_o from the wing apex were plotted against incidence in Fig.8 and against the lift coefficient in Fig.9. These figures show that at positive incidences C_m decreases as the sweepback angle of the trailing edge decreases. Fig.9 shows that the C_m characteristics for the trailing-edge sweepback angles of 5, -5 and -15 degrees are not evenly spaced; C_m does not decrease in direct proportion as the sweepback angle decreases because the effect of increased lift near the trailing edge is partially counterbalanced by that of the concurrent increase in the area and centre-line chord used to non-dimensionalize the pitching moment.

It has been demonstrated[2] that the pitching moment on a slender wing can be expressed as the sum of the effects of the linear normal force component acting through a point x_L from the wing apex and the non-linear normal force component acting through a point x_{NL} from the apex, i.e. that

$$C_m \cdot c_c = - C_{N_L} (x_L - 0.617\ c_o) - C_{N_{NL}} (x_{NL} - 0.617\ c_o) \quad .$$

The measured pitching moment characteristics for the three wings tested were analysed to find the effect of trailing-edge sweepback on x_L and x_{NL}.

The values of $\frac{C_m}{C_N}$ were calculated and plotted in Fig.10. Curves were then drawn through each set of plotted values to intercept the $\frac{C_m}{C_N}$ axis at $\left(\frac{C_m}{C_N}\right)_{\alpha=0}$ and the distance x_L from the apex to the point of action of the linear component of the normal force on each wing was found from the equation

$$\frac{x_L}{c_o} = 0.617 - \frac{c_c}{c_o}\left(\frac{C_m}{C_N}\right)_{\alpha=0} \quad .$$

Fig.11 shows that $\frac{x_L}{c_o}$ is not significantly affected by the trailing-edge sweepback angle; this conclusion is in accordance with the results obtained for the slightly cambered wings tested by Peckham[1]. For comparison the distance $\frac{\Delta h_L}{c_o}$ from the centre of area forward to the point of action of the linear component of the normal force on an ogee wing having a planform parameter $p = 0.469$, thickness/chord ratio $\frac{t}{c} = 0.04$ and a straight trailing edge was read from the correlating curves in Ref.2, corrected for the difference in

wing thickness and used to obtain a value of $\frac{x_L}{c_o}$ for $\phi = 0$. This calculated value corresponds closely with the value interpolated from the experimental results (see Fig.11).

The distance x_{NL} from the apex to the point of action of the non-linear component of the normal force on each wing was calculated from the equations

$$C_m c_c = - C_{N_L} (x_L - 0.617 c_o) - C_{N_{NL}} (x_{NL} - 0.617 c_o)$$

therefore

$$\frac{x_{NL}}{c_o} = 0.617 - \left\{ \frac{C_m}{\alpha} \frac{c_c}{c_o} + a \left(\frac{x_L}{c_o} - 0.617 \right) \right\} \Big/ \left(\frac{C_N}{\alpha} - a \right) .$$

The values of $\frac{x_{NL}}{c_o}$ were plotted in Fig.12 which shows that the point of action moves forward with increasing incidence because of the trailing-edge effect on the non-linear component and that the movement for each wing is similar to that measured[2] on wings with unswept trailing edges. Fig.13 shows that at large incidences, where the non-linear component has a significant effect, the parameter $\frac{\Delta h_{NL}}{c_o}$, where Δh_{NL} is the distance forward from the centre of area to the point of action, i.e. $\Delta h_{NL} = x_{ca} - x_{NL}$, is virtually unaffected by sweepback and is close to the value calculated from Ref.2.

3.5 Aerodynamic centre

The distance x_n from the apex to the aerodynamic centre was calculated for each wing from the equation

$$x_n = 0.617 c_o - \frac{dC_m}{dC_N} c_c ,$$

and the distance Δh_n from the centre of area forward to the aerodynamic centre from the equation

$$\Delta h_n = x_{ca} - x_n .$$

The values of $\frac{\Delta h_n}{c_o}$ were plotted in Fig.14 which shows that the distance Δh_n increases as the trailing-edge sweepback decreases. Fig.14 also shows that if Δh_n is non-dimensionalized with respect to the wing chord c_c then the value of $\frac{\Delta h_n}{c_c}$ is not greatly affected by trailing-edge sweepback, except at

small values of C_L. All the measured values of $\frac{\Delta h_n}{c_c}$ lie fairly close to the curve[2] correlating the results of wings with straight trailing edges, so the position of the aerodynamic centre on a wing with swept trailing edges can be estimated with reasonable accuracy by assuming $\frac{\Delta h_n(\phi)}{c_c(\phi)} = \frac{\Delta h_n(0)}{c_o}$, which can be obtained from the correlating curves in Ref.2.

4 CONCLUDING REMARKS

The results of this experiment suggest that, if the trailing-edge sweep-back of a slender wing is changed from zero to a small angle $\pm\phi$ deg, then

(1) C_{N_L} the linear component of the normal force coefficient

(2) $q\ S\ C_{N_{NL}}$ the non-linear component of the normal force

(3) K/A the ratio of the induced drag factor to the aspect ratio

(4) $\frac{x_L}{c_o}$ the distance from the apex to the point of action of C_{N_L}

(5) $\frac{\Delta h_{NL}}{c_o}$ the distance from the centre of area forward to the point of action of $C_{N_{NL}}$, and

(6) $\frac{\Delta h_n}{c_c}$ the distance from the centre of area forward to the aerodynamic centre

do not vary significantly. This being so, the lift, drag and pitching moment characteristics of a slender wing with swept trailing edges may be predicted with useful accuracy from the characteristics, obtainable from the correlating curves in Ref.2, of a wing with the same leading-edge shape and a straight trailing edge.

Table 1

DETAILS OF WINGS TESTED

Trailing-edge sweepback angle ϕ, deg	5	-5	-15
Semispan b/2, ft	0.582	0.582	0.582
Centre-line chord c_c, ft	1.688	1.790	1.895
Area S, sq ft	0.9175	0.9769	1.0378
Maximum thickness/chord ratio	0.03	0.03	0.03
Slenderness ratio $b/2\ c_c$	0.345	0.325	0.307
Aspect ratio A	1.476	1.387	1.305
Modified aspect ratio $A\ (1 + c_{0.99}/c_c)$	1.538	1.443	1.355
Planform parameter $p = S/b\ c_c$	0.468	0.470	0.472

Table 2

MEASURED AERODYNAMIC CHARACTERISTICS ($\phi = +5^{o}$)

α_{deg}	C_L	C_D	C_N	C_A	$C_{m_{0.617\ c_o}}$	$\frac{C_N}{\alpha}$	K
							$C_{D_o} = 0.0048$
-4.88	-0.1694	0.0166	-0.1702	0.0021	0.00501	1.996	
-4.37	-0.1486	0.0140	-0.1493	0.0026	0.00429	1.957	
-3.85	-0.1285	0.0118	-0.1290	0.0031	0.00375	1.917	
-3.34	-0.1100	0.0097	-0.1104	0.0033	0.00323	1.893	
-2.83	-0.0916	0.0082	-0.0919	0.0036	0.00285	1.863	
-2.31	-0.0735	0.0072	-0.0738	0.0042	0.00200	1.826	
-1.80	-0.0571	0.0062	-0.0572	0.0044	0.00154	1.820	
-1.29	-0.0409	0.0050	-0.0410	0.0041	0.00114	1.822	
-0.78	-0.0205	0.0044	-0.0205	0.0041	0.00062	1.518	
-0.26	-0.0043	0.0042	-0.0043	0.0042	+0.00022	0.944	
+0.25	+0.0076	0.0040	+0.0094	0.0040	-0.00010	2.154	
0.76	0.0210	0.0042	0.0210	0.0039	-0.00041	1.595	
1.27	0.0370	0.0048	0.0371	0.0039	-0.00129	1.679	
1.78	0.0574	0.0063	0.0576	0.0045	-0.00153	1.852	
2.29	0.0732	0.0069	0.0734	0.0040	-0.00195	1.834	1.811
2.81	0.0911	0.0082	0.0914	0.0037	-0.00248	1.865	1.874
3.32	0.1100	0.0096	0.1104	0.0032	-0.00313	1.905	1.843
3.84	0.1306	0.0117	0.1311	0.0029	-0.00368	1.958	1.866
4.35	0.1501	0.0141	0.1507	0.0027	-0.00418	1.985	1.911
4.87	0.1707	0.0171	0.1715	0.0026	-0.00462	2.020	1.962
5.38	0.1903	0.0198	0.1913	0.0018	-0.00515	2.037	1.914
6.41	0.2342	0.0275	0.2358	0.0012	-0.00605	2.107	1.918
7.45	0.2827	0.0378	0.2852	0.0009	-0.00716	2.194	1.917
8.48	0.3299	0.0494	0.3335	0.0002	-0.00767	2.253	1.903
9.52	0.3764	0.0630	0.3817	-0.0001	-0.00803	2.298	1.905
10.46	0.4204	0.0782	0.4276	0.0006	-0.00822	2.343	1.927
11.59	0.4716	0.0959	0.4813	-0.0007	-0.00803	2.380	1.900
12.62	0.5210	0.1155	0.5337	-0.0012	-0.00780	2.422	1.891
13.66	0.5710	0.1365	0.5871	-0.0022	-0.00728	2.463	1.873
14.75	0.6200	0.1598	0.6403	-0.0033	-0.00655	2.488	1.869
15.74	0.6722	0.1861	0.6970	-0.0033	-0.00613	2.537	1.861
16.77	0.7242	0.2145	0.7553	-0.0036	-0.00537	2.580	1.854
17.81	0.7763	0.2454	0.8142	-0.0039	-0.00456	2.619	1.851
18.85	0.8286	0.2779	0.8739	-0.0047	-0.00359	2.656	1.845
19.89	0.8745	0.3093	0.9276	-0.0066	-0.00241	2.673	1.846
20.93	0.9270	0.3469	0.9897	-0.0071	-0.00104	2.710	1.846
21.96	0.9745	0.3841	1.0474	-0.0082	+0.00027	2.733	1.852
23.00	1.0262	0.4260	1.1111	-0.0088	0.00186	2.768	1.855
24.04	1.0770	0.4715	1.1756	-0.0081	0.00360	2.803	1.866
25.07	1.1155	0.5078	1.2255	-0.0126	0.00533	2.801	1.874
26.10	1.1652	0.5580	1.2919	-0.0116	0.00722	2.836	1.890

Table 3

MEASURED AERODYNAMIC CHARACTERISTICS ($\phi = -5^{o}$)

α_{deg}	C_L	C_D	C_N	C_A	$C_{m_{0.617\ c_o}}$	$\frac{C_N}{\alpha}$	K
							$C_{D_o} = 0.0053$
-4.94	-0.1658	0.0173	-0.1667	0.0030	0.00597	1.933	
-4.43	-0.1462	0.0147	-0.1469	0.0034	0.00522	1.902	
-3.91	-0.1280	0.0124	-0.1285	0.0037	0.00473	1.883	
-3.40	-0.1097	0.0104	-0.1101	0.0039	0.00410	1.857	
-2.88	-0.0918	0.0089	-0.0922	0.0042	0.00338	1.832	
-2.37	-0.0755	0.0079	-0.0758	0.0047	0.00279	1.832	
-1.86	-0.0591	0.0068	-0.0593	0.0049	0.00242	1.829	
-1.34	-0.0403	0.0050	-0.0404	0.0041	0.00150	1.725	
-0.83	-0.0235	0.0046	-0.0236	0.0043	0.00066	1.632	
-0.32	-0.0090	0.0045	-0.0090	0.0044	0.00020	1.626	
+0.19	+0.0041	0.0045	+0.0041	0.0045	+0.00024	1.237	
0.70	0.0173	0.0045	0.0174	0.0043	-0.00050	1.415	
1.22	0.0325	0.0049	0.0326	0.0042	-0.00108	1.536	
1.73	0.0524	0.0064	0.0525	0.0048	-0.00237	1.739	
2.24	0.0677	0.0071	0.0679	0.0045	-0.00266	1.734	
2.76	0.0845	0.0083	0.0848	0.0042	-0.00326	1.762	1.818
3.27	0.1065	0.0100	0.1069	0.0039	-0.00377	1.870	1.817
3.79	0.1251	0.0119	0.1256	0.0036	-0.00407	1.900	1.826
4.30	0.1442	0.0142	0.1449	0.0033	-0.00492	1.929	1.867
4.82	0.1639	0.0170	0.1647	0.0031	-0.00551	1.958	1.892
5.34	0.1845	0.0201	0.1855	0.0028	-0.00629	1.991	1.895
6.37	0.2270	0.0275	0.2286	0.0022	-0.00741	2.057	1.878
7.40	0.2692	0.0364	0.2716	0.0014	-0.00861	2.102	1.869
8.44	0.3154	0.0477	0.3189	0.0008	-0.00967	2.165	1.855
9.48	0.3625	0.0607	0.3675	0.0002	-0.01068	2.222	1.837
10.52	0.4102	0.0762	0.4173	0.0001	-0.01210	2.274	1.838
11.55	0.4581	0.0937	0.4675	0	-0.01257	2.319	1.836
12.59	0.5091	0.1134	0.5216	-0.0003	-0.01271	2.373	1.819
13.63	0.5588	0.1347	0.5748	-0.0008	-0.01307	2.416	1.806
14.67	0.6100	0.1584	0.6302	-0.0013	-0.01344	2.461	1.793
15.71	0.6601	0.1835	0.6851	-0.0021	-0.01355	2.498	1.783
16.75	0.7053	0.2075	0.7352	-0.0046	-0.01339	2.515	1.772
17.79	0.7574	0.2381	0.7939	-0.0047	-0.01356	2.557	1.769
18.83	0.8098	0.2709	0.8539	-0.0050	-0.01362	2.598	1.765
19.88	0.8622	0.3057	0.9148	-0.0056	-0.01335	2.637	1.761
20.92	0.9146	0.3429	0.9767	-0.0062	-0.01304	2.675	1.759
21.96	0.9654	0.3829	1.0385	-0.0059	-0.01269	2.710	1.766
23.00	1.0168	0.4244	1.1018	-0.0066	-0.01212	2.745	1.767
24.04	1.0675	0.4692	1.1660	-0.0064	-0.01155	2.779	1.774
25.08	1.1174	0.5175	1.2314	-0.0050	-0.01087	2.813	1.788
26.12	1.1620	0.5614	1.2905	-0.0075	-0.01000	2.831	1.795

Table 4

MEASURED AERODYNAMIC CHARACTERISTICS ($\phi = -15^{o}$)

α_{deg}	C_L	C_D	C_N	C_A	$C_{m_{0.617\ c_o}}$	$\frac{C_N}{\alpha}$	K
							$C_{D_o} = 0.0044$
-4.81	-0.1585	0.0158	-0.1593	0.0025	0.00535	1.894	
-4.29	-0.1427	0.0137	-0.1433	0.0030	0.00489	1.910	
-3.78	-0.1228	0.0113	-0.1233	0.0032	0.00424	1.864	
-3.26	-0.1032	0.0094	-0.1036	0.0035	0.00341	1.815	
-2.74	-0.0850	0.0079	-0.0853	0.0038	0.00295	1.777	
-2.23	-0.0685	0.0068	-0.0687	0.0041	0.00224	1.757	
-1.71	-0.0517	0.0059	-0.0519	0.0043	0.00174	1.729	
-1.20	-0.0367	0.0047	-0.0368	0.0039	0.00133	1.743	
-0.69	-0.0206	0.0038	-0.0206	0.0035	0.00097	1.686	
-0.17	-0.0050	0.0037	-0.0050	0.0037	+0.00023	1.592	
+0.34	+0.0100	0.0038	+0.0100	0.0036	-0.00018	1.685	
0.85	0.0250	0.0038	0.0250	0.0035	-0.00087	1.705	
1.36	0.0399	0.0047	0.0400	0.0037	-0.00133	1.698	
1.88	0.0558	0.0056	0.0560	0.0038	-0.00190	1.716	1.581
2.39	0.0722	0.0065	0.0724	0.0035	-0.00246	1.743	1.675
2.91	0.0894	0.0077	0.0897	0.0032	-0.00314	1.772	1.700
3.42	0.1081	0.0093	0.1085	0.0028	-0.00388	1.823	1.725
3.94	0.1268	0.0112	0.1272	0.0025	-0.00454	1.855	1.746
4.46	0.1462	0.0137	0.1468	0.0023	-0.00517	1.890	1.778
4.97	0.1663	0.0164	0.1671	0.0019	-0.00585	1.930	1.780
5.49	0.1825	0.0189	0.1835	0.0014	-0.00635	1.915	1.782
6.52	0.2213	0.0257	0.2228	0.0004	-0.00739	1.961	1.782
7.56	0.2673	0.0354	0.2696	-0.0001	-0.00879	2.046	1.778
8.60	0.3156	0.0472	0.3191	-0.0005	-0.01034	2.129	1.762
9.64	0.3569	0.0589	0.3617	-0.0017	-0.01157	2.152	1.754
10.67	0.3985	0.0720	0.4050	-0.0031	-0.01264	2.177	1.744
11.71	0.4474	0.0893	0.4562	-0.0034	-0.01368	2.234	1.739
12.75	0.4922	0.1065	0.5036	-0.0048	-0.01411	2.265	1.727
13.79	0.5410	0.1265	0.5555	-0.0061	-0.01527	2.310	1.711
14.84	0.5935	0.1508	0.6124	-0.0062	-0.01636	2.366	1.704
15.88	0.6420	0.1740	0.6651	-0.0083	-0.01719	2.401	1.687
16.93	0.6950	0.2024	0.7238	-0.0087	-0.01812	2.451	1.680
17.97	0.7415	0.2290	0.7779	-0.0051	-0.01882	2.482	1.675
19.01	0.7896	0.2579	0.8306	-0.0133	-0.01935	2.505	1.667
20.06	0.8424	0.2930	0.8918	-0.0137	-0.01994	2.549	1.667
21.10	0.8966	0.3311	0.9556	-0.0139	-0.02090	2.595	1.666
22.15	0.9464	0.3687	1.0154	-0.0151	-0.02082	2.627	1.669
23.18	0.9903	0.4036	1.0692	-0.0189	-0.02088	2.644	1.669
24.22	1.0367	0.4431	1.1272	-0.0213	-0.02092	2.668	1.674
25.27	1.0899	0.4910	1.1952	-0.0213	-0.02126	2.711	1.679
26.31	1.1313	0.5313	1.2496	-0.0251	-0.02112	2.722	1.688

Table 5

LINEAR AND NON-LINEAR COMPONENTS OF NORMAL FORCE

ϕ / α	5			-5			-15		
	$\frac{C_N}{\alpha}$	$\frac{C_N}{\alpha} - a$	$\frac{C_N/\alpha - a}{A}$	$\frac{C_N}{\alpha}$	$\frac{C_N}{\alpha} - a$	$\frac{C_N/\alpha - a}{A}$	$\frac{C_N}{\alpha}$	$\frac{C_N}{\alpha} - a$	$\frac{C_N/\alpha - a}{A}$
0	1.64	0	0	1.63	0	0	1.62	0	0
4	1.94	0.30	0.203	1.90	0.27	0.195	1.86	0.24	0.183
8	2.21	0.57	0.386	2.14	0.51	0.368	2.07	0.45	0.345
12	2.40	0.76	0.515	2.34	0.71	0.512	2.24	0.62	0.475
16	2.55	0.91	0.617	2.50	0.87	0.627	2.41	0.79	0.605
20	2.68	1.04	0.705	2.64	1.01	0.728	2.55	0.93	0.712
24	2.79	1.15	0.780	2.78	1.15	0.829	2.67	1.05	0.804

Table 6

CENTRES OF LINEAR AND NON-LINEAR NORMAL FORCE

ϕ	α deg	$\frac{C_m}{C_N}$	$\frac{x_L}{c_o}$	$\frac{C_m}{\alpha}$	$\frac{x_{NL}}{c_o}$	$\frac{x_{ca}}{c_o}$	$\frac{\Delta h_{NL}}{c_o}$
5	0	-0.030	0.646			0.682	
	8			-0.0537	0.625		0.057
	12			-0.0396	0.604		0.078
	16			-0.0215	0.587		0.095
	20			-0.0072	0.578		0.104
	24			+0.0084	0.568		0.114
-5	0	-0.035	0.653			0.701	
	8			-0.0652	0.633		0.068
	12			-0.0582	0.619		0.082
	16			-0.0480	0.606		0.095
	20			-0.0380	0.597		0.104
	24			-0.0274	0.590		0.111
-15	0	-0.036	0.656			0.721	
	8			-0.0710	0.648		0.073
	12			-0.0665	0.631		0.090
	16			-0.0626	0.623		0.097
	20			-0.0573	0.616		0.105
	24			-0.0506	0.611		0.110

Table 7

AERODYNAMIC CENTRE POSITIONS

ϕ	C_N	$\frac{dC_m}{dC_N}$	$\frac{x_n}{c_o}$	$\frac{x_{ca}}{c_o}$	$\frac{\Delta h_n}{c_o}$	$\frac{\Delta h_n}{c_o}$
5	0.2	-0.022	0.638	0.682	0.044	0.045
	0.4	-0.003	0.620		0.062	0.064
	0.6	+0.009	0.608		0.074	0.076
	0.8	+0.016	0.601		0.081	0.083
	1.0	+0.023	0.595		0.087	0.090
-5	0.2	-0.029	0.647	0.701	0.054	0.052
	0.4	-0.016	0.633		0.068	0.065
	0.6	-0.004	0.621		0.080	0.077
	0.8	0	0.617		0.084	0.081
	1.0	+0.006	0.611		0.090	0.087
-15	0.2	-0.032	0.652	0.721	0.069	0.063
	0.4	-0.023	0.642		0.079	0.072
	0.6	-0.016	0.634		0.087	0.080
	0.8	-0.012	0.629		0.092	0.084
	1.0	-0.007	0.624		0.097	0.089

SYMBOLS

A	aspect ratio
a	$dC_N/d\alpha$ at zero incidence
b	wing span
C_D	drag coefficient
C_{D_o}	drag coefficient at zero lift
C_L	lift coefficient
C_m	pitching moment coefficient, about $x = 0.617\ c_o$
C_N	normal force coefficient
C_{N_L}	linear component of the normal force coefficient
$C_{N_{NL}}$	non-linear component of the normal force coefficient
c	local wing chord
c_c	centre-line chord
c_o	centre-line chord for $\phi = 0$
$c_{0.99}$	wing chord at $y = 0.99\ b/2$
Δh_n	$x_{ca} - x_n$
Δh_{NL}	$x_{ca} - x_{NL}$
K	lift-dependent drag factor
L	lift
p	planform parameter, $\frac{S}{b\ c_c}$
q	dynamic pressure
S	wing plan area
t/c	thickness/chord ratio
x,y,z	orthogonal coordinates; x measured in chordal plane downstream from the wing apex, y measured perpendicular to the freestream, and z measured perpendicular to the chordal plane
x'	chordwise distance from the leading edge
x_{ca}	distance from apex to centre of area
x_L	distance from apex to point of action of C_{N_L}
x_n	distance from apex to aerodynamic centre

REFERENCES

No.	Author	Title, etc.
1	D.H. Peckham	Low speed wind tunnel tests on a series of uncambered slender pointed wings with sharp edges. A.R.C. R. & M. 3186 (1958)
2	D.A. Kirby	An experimental investigation of the effect of plan-form shape on the subsonic longitudinal stability characteristics of slender wings. A.R.C. R. & M. 3568 (1967)
3	R.C. Pankhurst D.W. Holder	Wind-tunnel technique, Chapter 8. Pitman, London 1948
4	H.C. Garner E.W.E. Rogers W.E.A. Acum E.C. Maskell	Subsonic wind-tunnel wall corrections. AGARDograph 109, October 1966

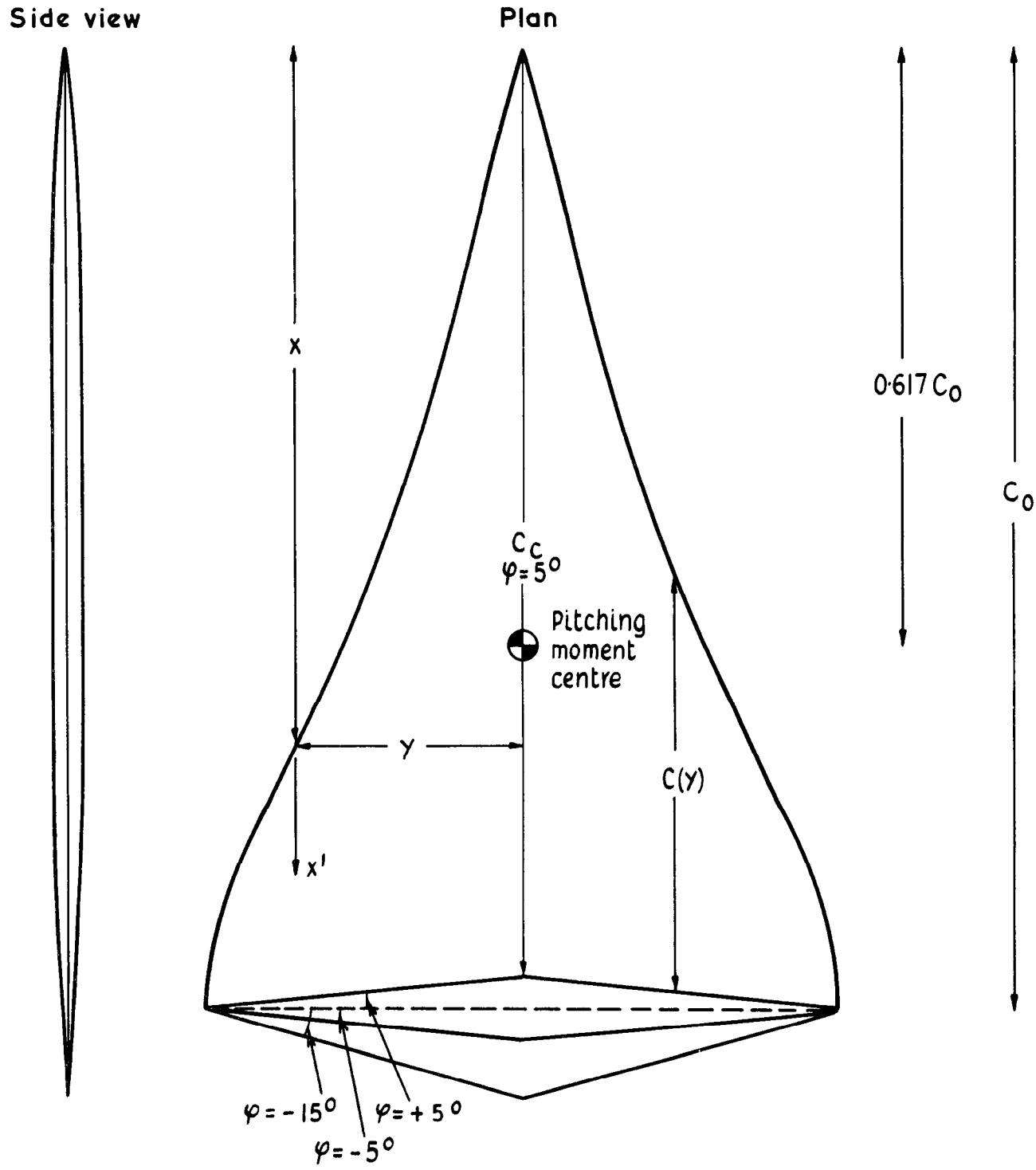

Fig.1 Wing planforms and notation

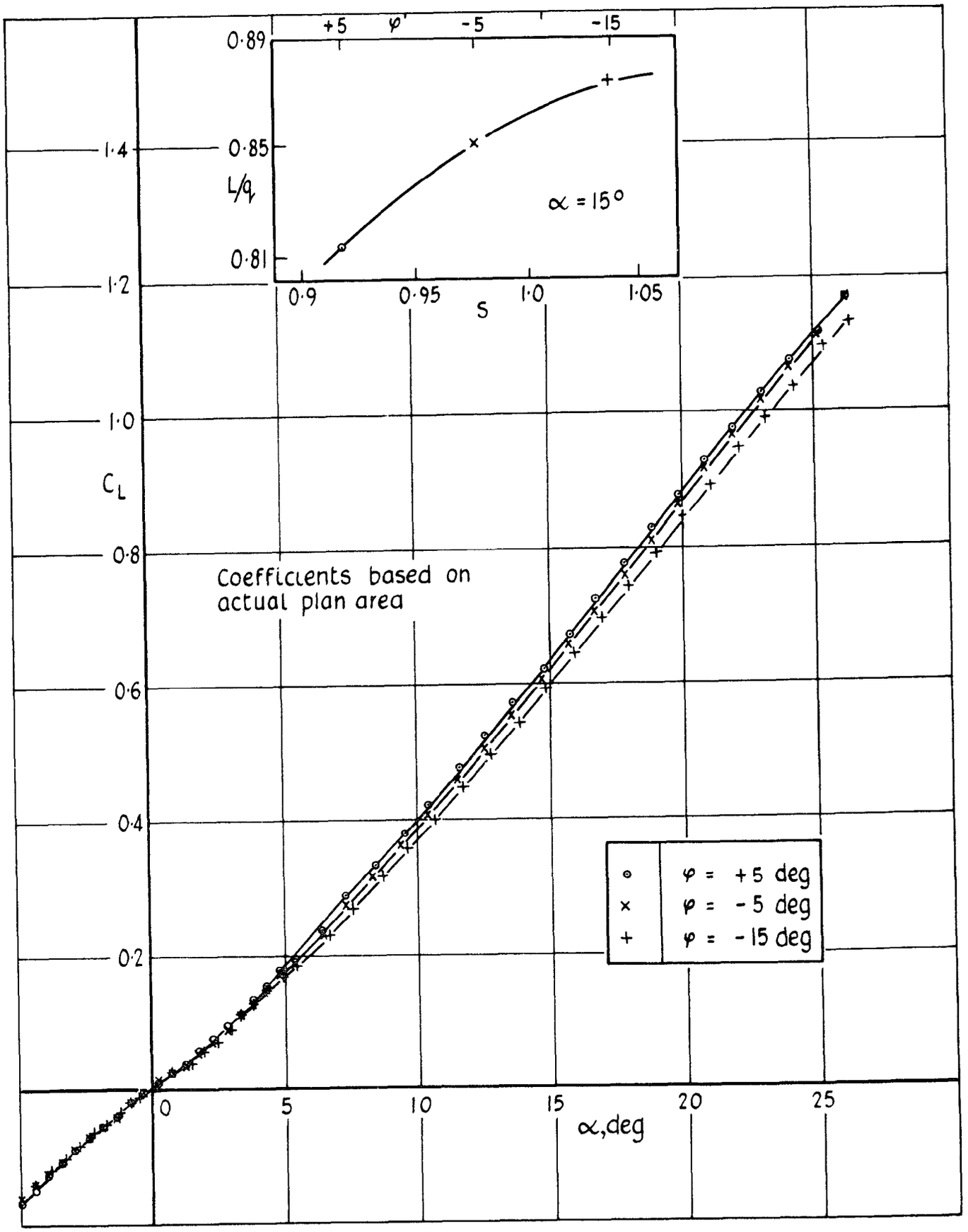

Fig. 2 Effect of trailing-edge sweepback on lift coefficient

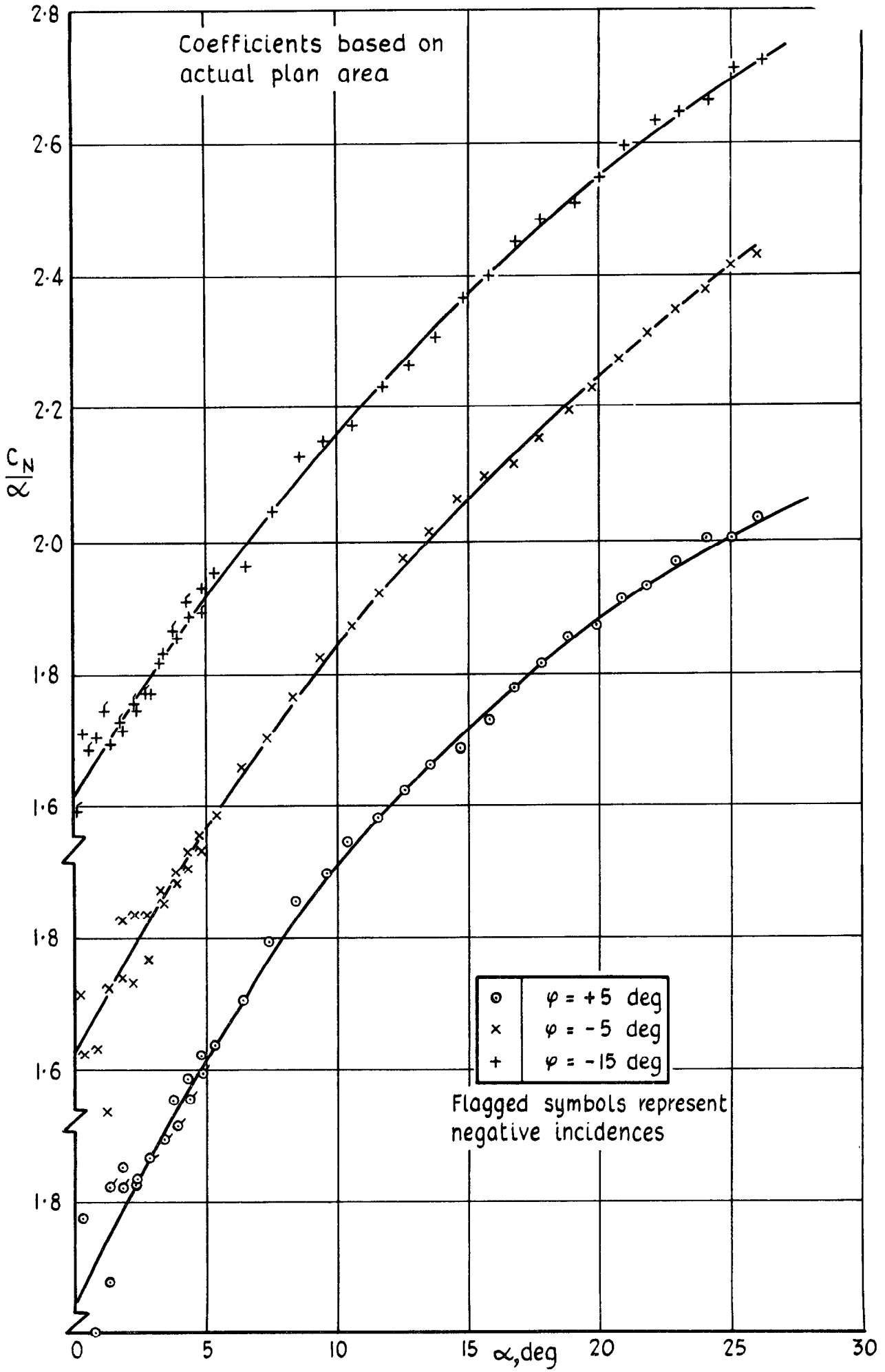

Fig.3 Effect of trailing-edge sweepback on normal force

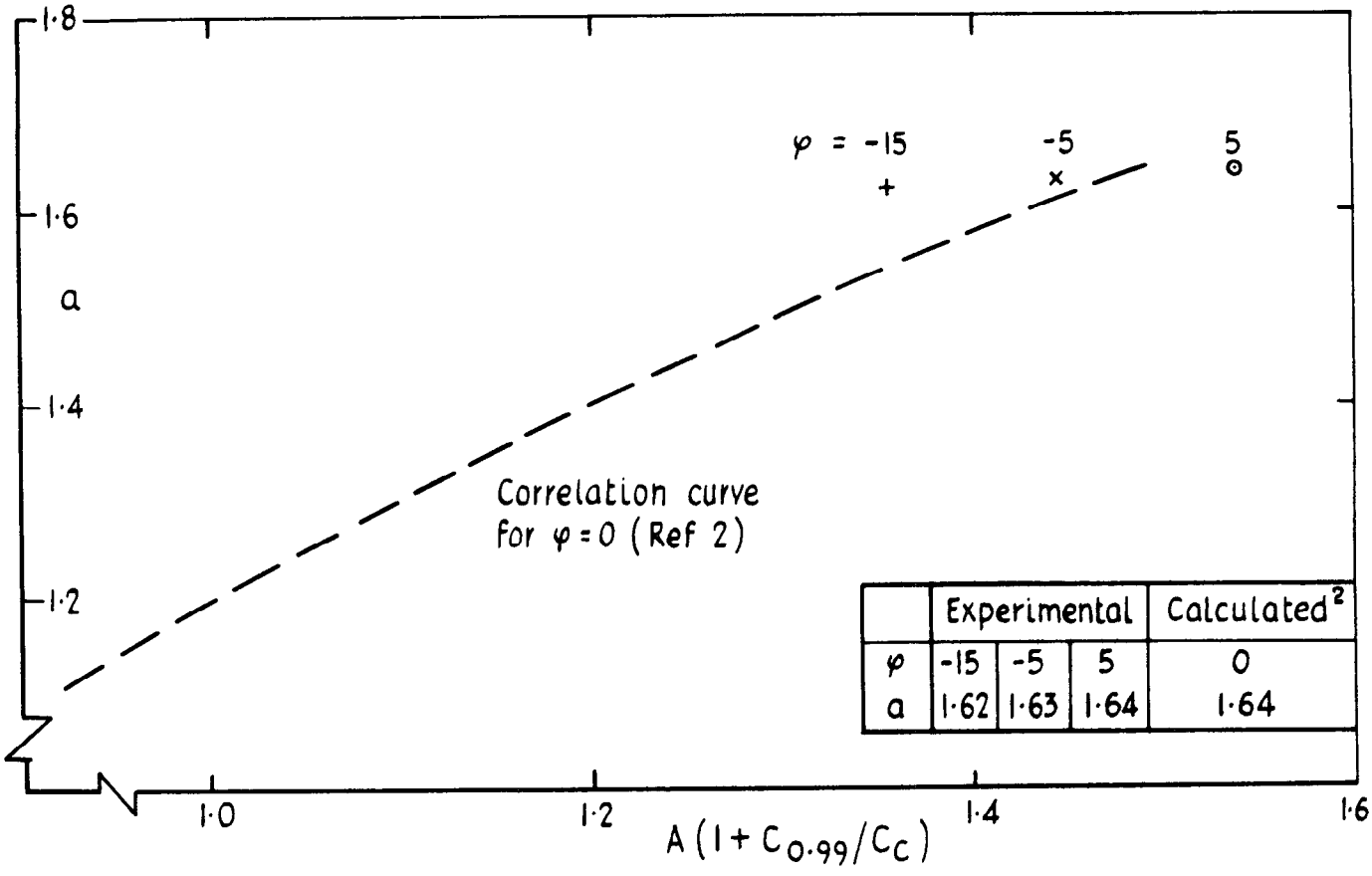

	Experimental			Calculated[2]
φ	-15	-5	5	0
a	1·62	1·63	1·64	1·64

Fig. 4 Effect of sweepback on linear component

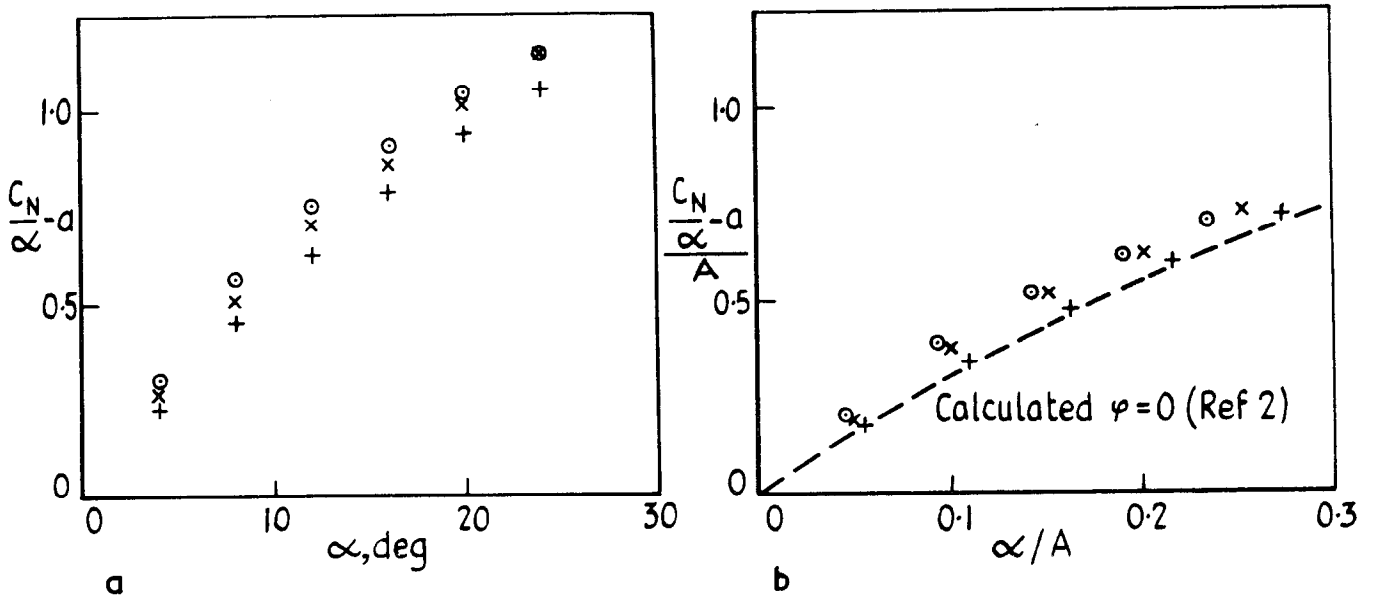

Fig. 5a & b Effect of sweepback on non-linear component

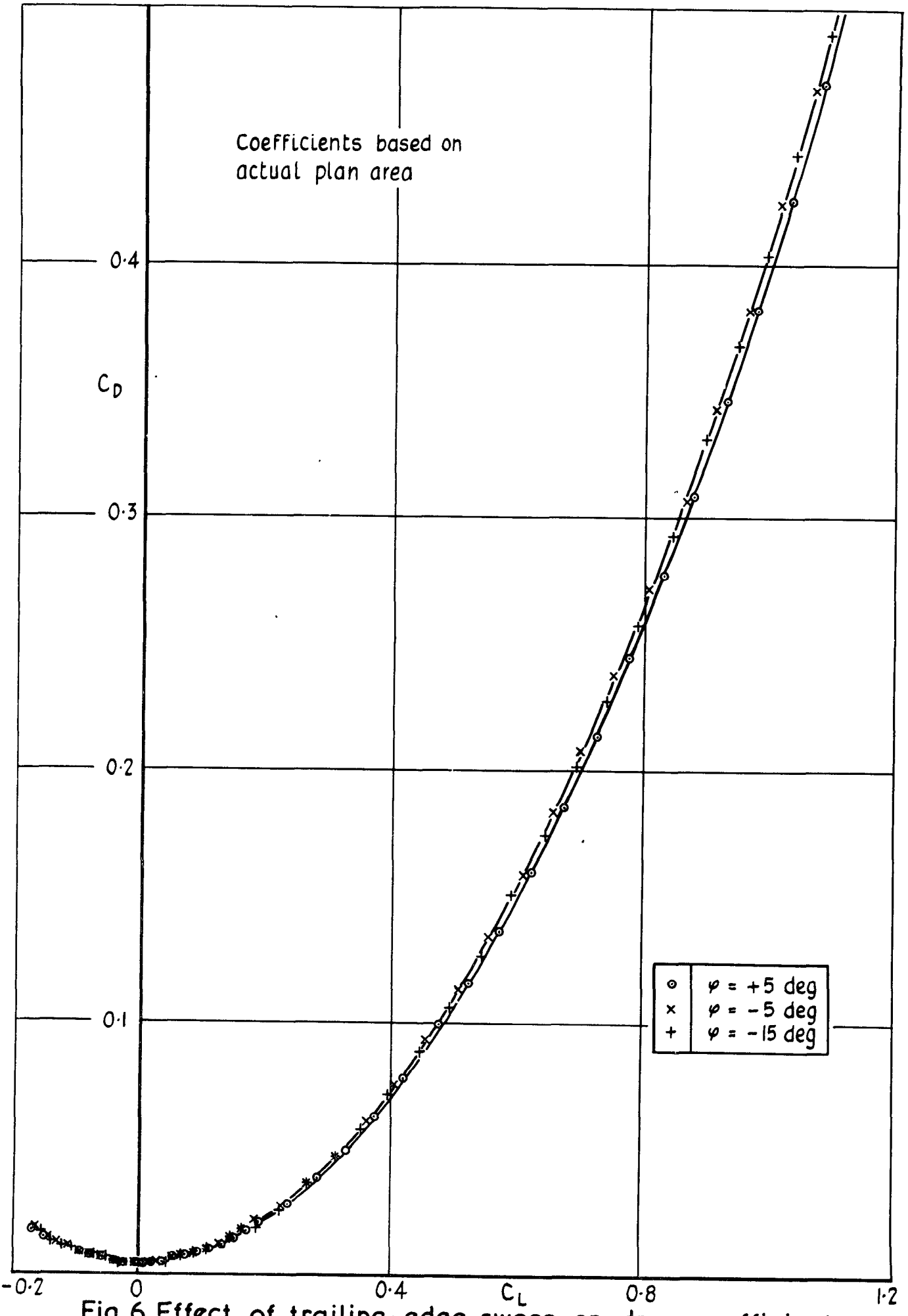

Fig.6 Effect of trailing-edge sweep on drag coefficient

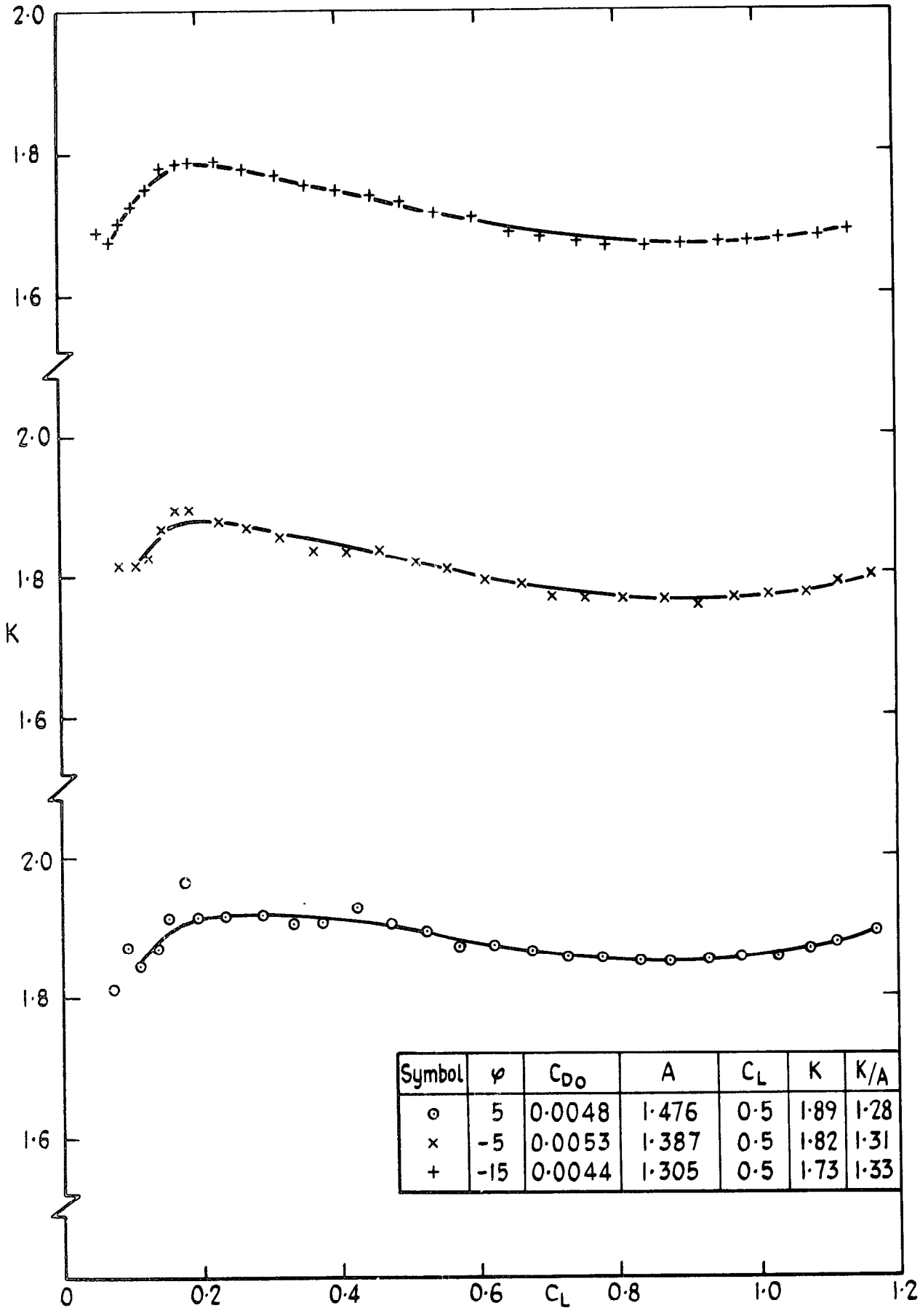

Fig.7 Effect of trailing-edge sweepback on the lift-dependant drag factor

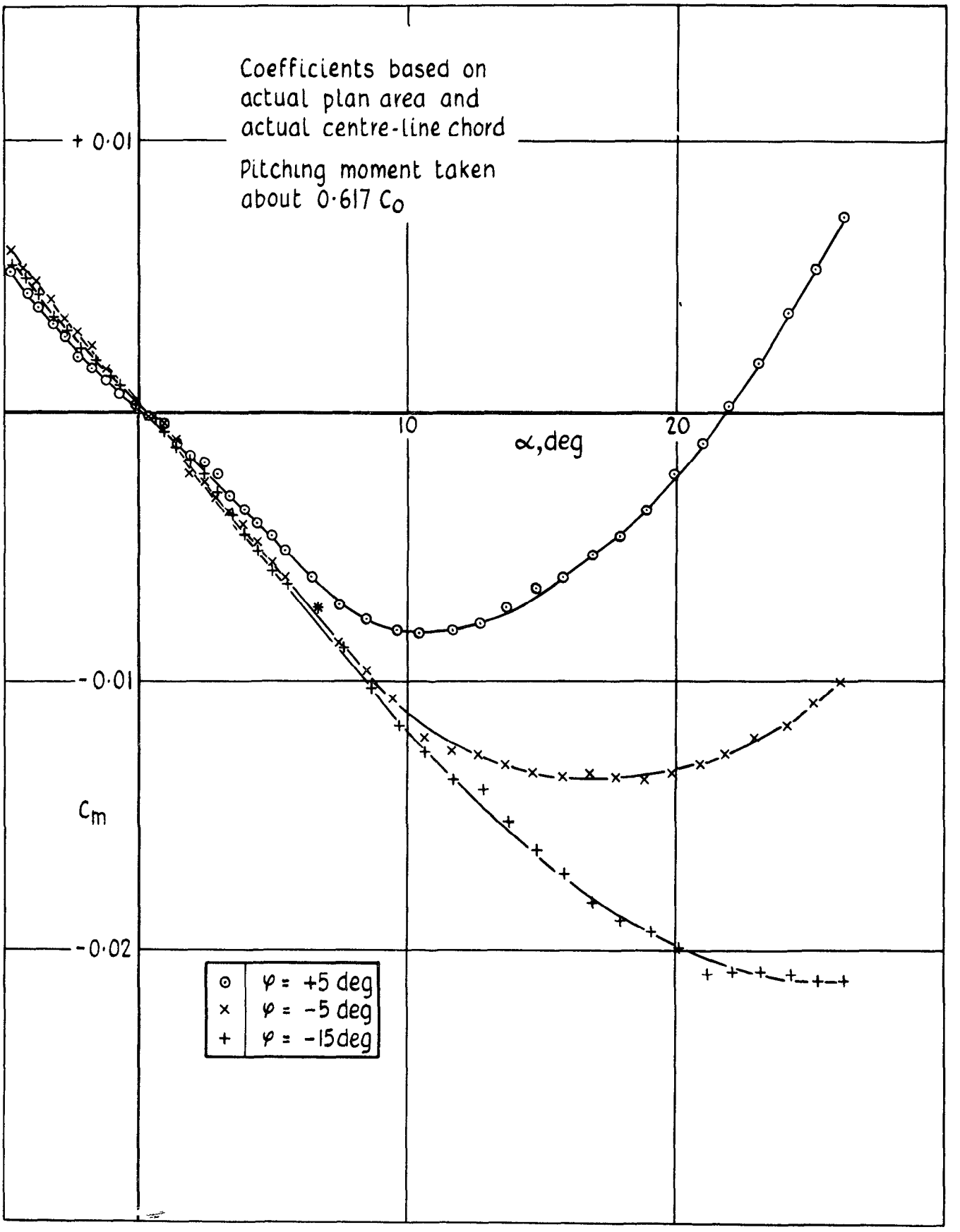

Fig.8 Effect of trailing-edge sweepback on pitching moment coefficient

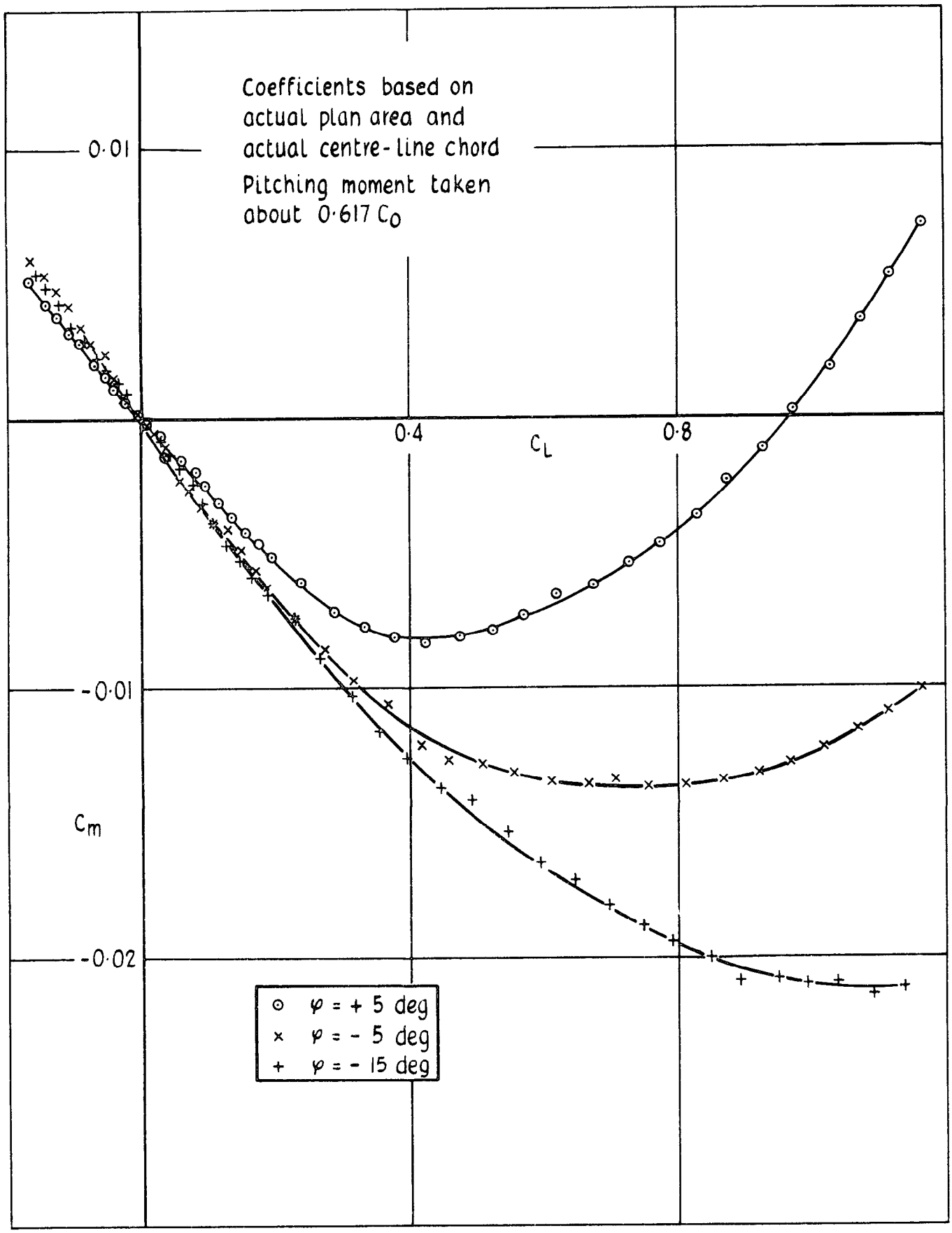

Fig. 9 Effect of trailing-edge sweepback on pitching moment coefficient

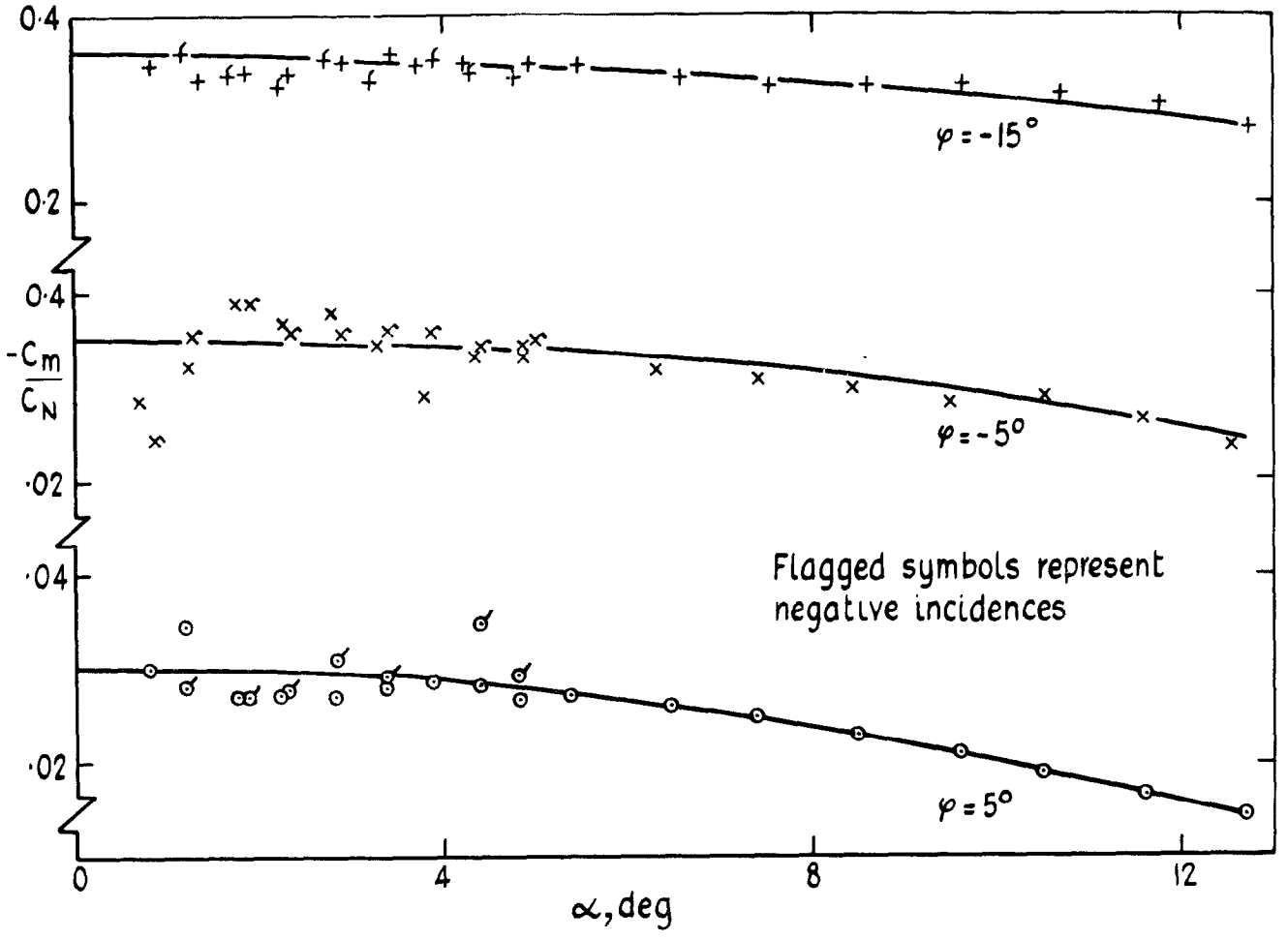

Fig.10 Variation with incidence of C_m/C_N

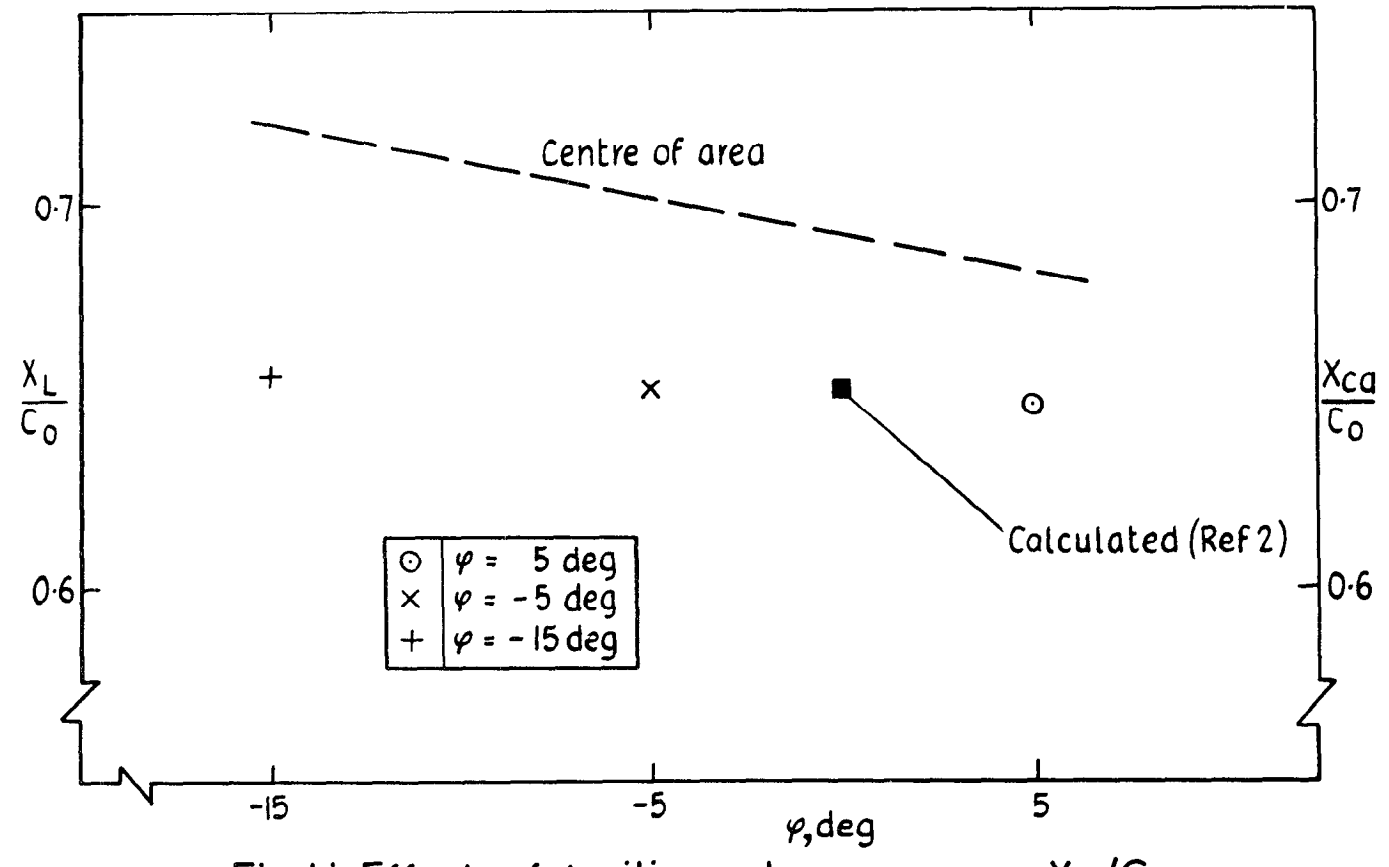

Fig.11 Effect of trailing-edge sweep on X_L/C_O

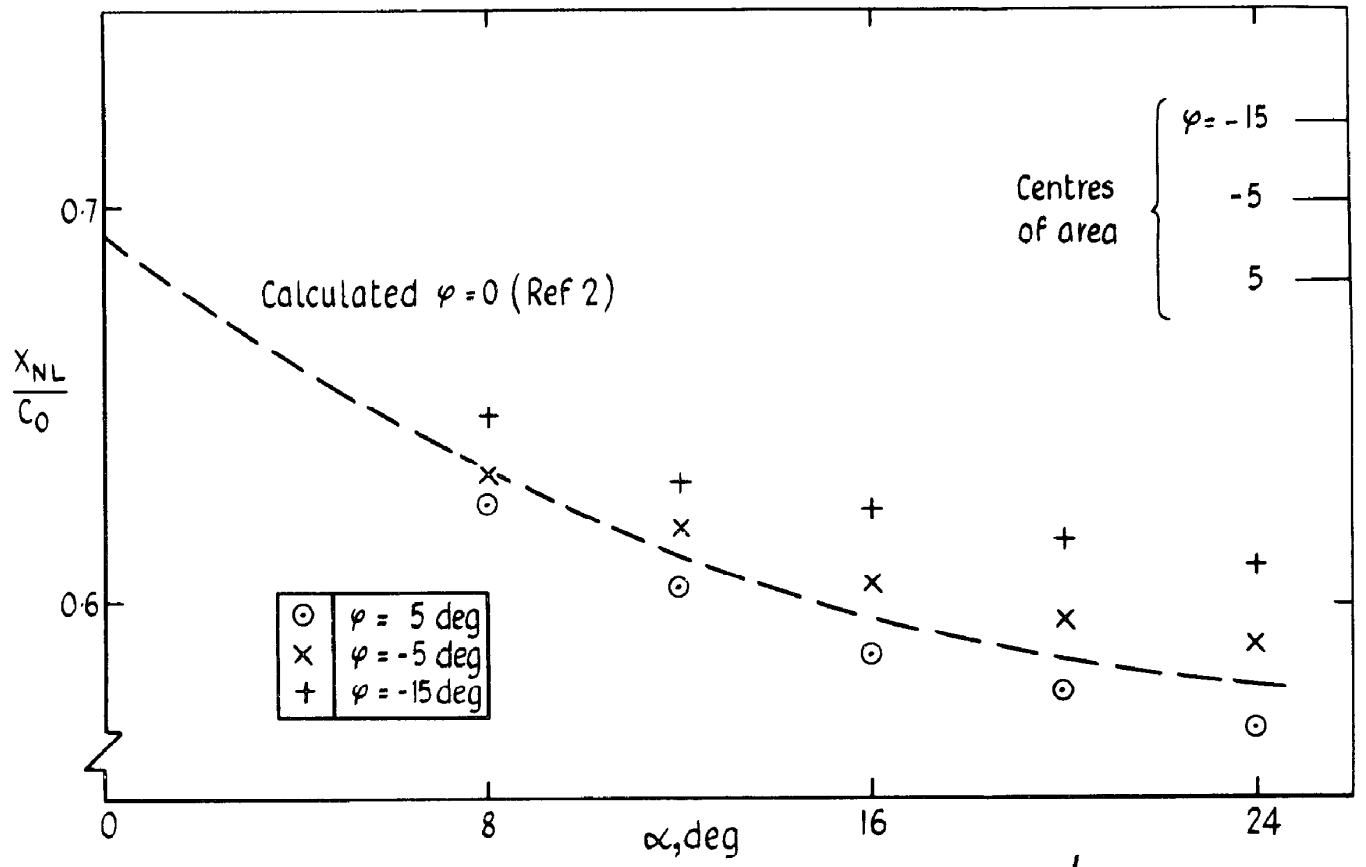

Fig.12 Variation with incidence of X_{NL}/C_O

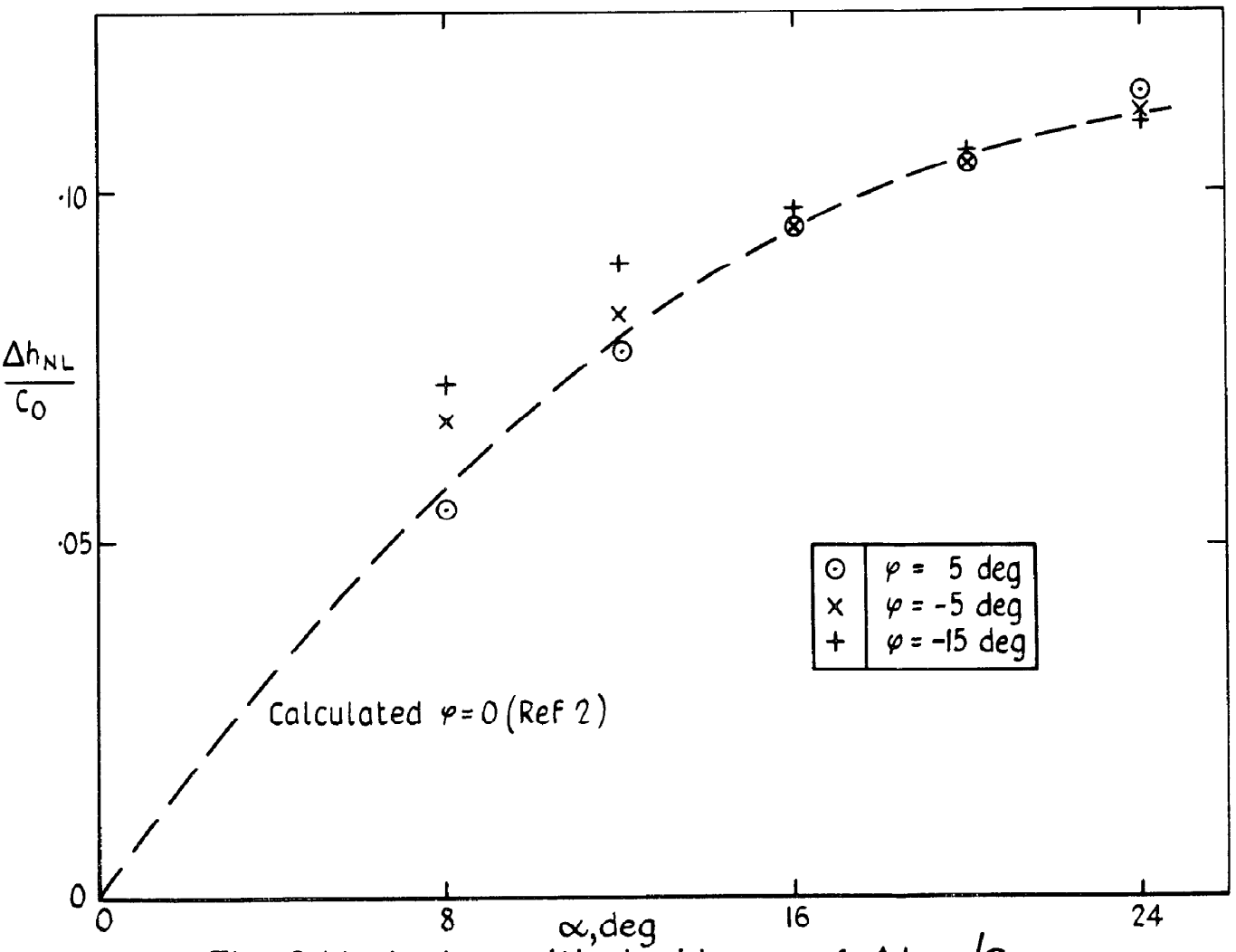

Fig.13 Variation with incidence of $\Delta h_{NL}/C_O$

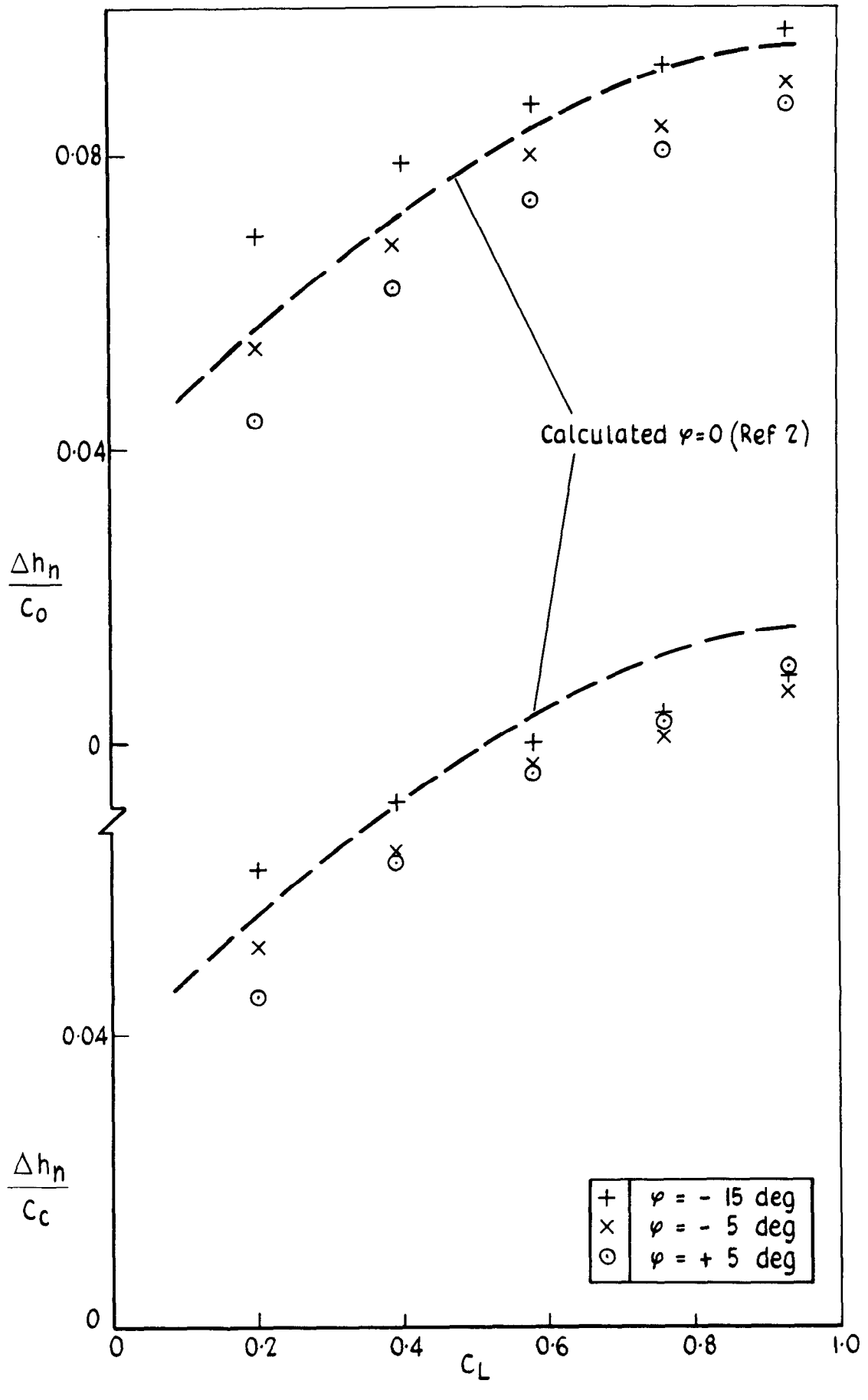

Fig.14 Variation of Δh_n with C_L

Printed in England for Her Majesty's Stationery Office by the Royal Aircraft Establishment, Farnborough. Dd.501371. K.4.

A.R.C. C.P. No. 1130
March 1970

Kirkpatrick, D. L. I.
Hepworth, A. G.

EXPERIMENTAL INVESTIGATION OF THE EFFECT OF TRAILING-EDGE SWEEPBACK ON THE SUBSONIC LONGITUDINAL CHARACTERISTICS OF SLENDER WING

533.693.3 :
533.6.013.412 :
533.691.2 :
533.6.013.12 :
533.6.013.13 :
533.6.013.152 :
533.6.011.32

This Report presents the results of an experiment to measure the lift, drag and pitching moment characteristics of three slender ogee wings with different trailing-edge sweepback angles. Analysis of these results shows how the characteristics of wings with swept trailing edges can be correlated with those of wings with unswept trailing edges.

A.R.C. C.P. No. 1130
March 1970

Kirkpatrick, D. L. I.
Hepworth, A. G.

EXPERIMENTAL INVESTIGATION OF THE EFFECT OF TRAILING-EDGE SWEEPBACK ON THE SUBSONIC LONGITUDINAL CHARACTERISTICS OF SLENDER WING

533.693.3 :
533.6.013.412 :
533.691.2 :
533.6.013.12 :
533.6.013.13 :
533.6.013.152 :
533.6.011.32

This Report presents the results of an experiment to measure the lift, drag and pitching moment characteristics of three slender ogee wings with different trailing-edge sweepback angles. Analysis of these results shows how the characteristics of wings with swept trailing edges can be correlated with those of wings with unswept trailing edges.

DETACHABLE ABSTRACT CARD

A.R.C. C.P. No. 1130
March 1970

Kirkpatrick, D. L. I.
Hepworth, A. G.

EXPERIMENTAL INVESTIGATION OF THE EFFECT OF TRAILING-EDGE SWEEPBACK ON THE SUBSONIC LONGITUDINAL CHARACTERISTICS OF SLENDER WINGS

533.693.3 :
533.6.013.412 :
533.691.2 :
533.6.013.12 :
533.6.013.13 :
533.6.013.152 :
533.6.011.32

This Report presents the results of an experiment to measure the lift, drag and pitching moment characteristics of three slender ogee wings with different trailing-edge sweepback angles. Analysis of these results shows how the characteristics of wings with swept trailing edges can be correlated with those of wings with unswept trailing edges.

Published by
HER MAJESTY'S STATIONERY OFFICE

To be purchased from
49 High Holborn, London W.C.1
13a Castle Street, Edinburgh EH2 3AR
109 St. Mary Street, Cardiff CF1 1JW
Brazennose Street, Manchester 2
50 Fairfax Street, Bristol BS1 3DE
258 Broad Street, Birmingham 1
7 Linenhall Street, Belfast BT2 8AY
or through any bookseller

C.P. No. 1130

SBN 11 470318 3